MAX PLANCK INSTITUTE
FOR PHYSICS

Klaus Tschira
Stiftung

O$\nu$DES
Project

# O$\nu$DES - Probing Solar Neutrino BSM Physics with Cryogenic Scintillating Calorimeters

Elisa Gaido
Max Planck Institute for Physics

TeVPA 2026 (Tendō, Japan) - September 3, 2026

# Overview

1. **Introduction: The O$\nu$DES program**
2. **$\nu$-e scattering**
3. **Proof-of-principle prototype**
4. **Conclusions**

# Motivation

COSINUS aims to cross-check the DAMA/LIBRA claim for DM-nucleus scattering

**Check out the COSINUS overview talk by M. Bharadwaj on Sep. 2 at 2 pm!**

# Motivation

COSINUS aims to cross-check the DAMA/LIBRA claim for DM-nucleus scattering

How can we use the same technology to cross-check DAMA/LIBRA for DM-electron interactions?

# Motivation

COSINUS aims to cross-check the DAMA/LIBRA claim for DM-nucleus scattering

How can we use the same technology to cross-check DAMA/LIBRA for DM-electron interactions?

**O$\nu$DES Project**

**O**bservatory for **N**eutrino and **D**ark matter **E**lectron **S**cattering

# Motivation

COSINUS aims to cross-check the DAMA/LIBRA claim for DM-nucleus scattering

How can we use the same technology to cross-check DAMA/LIBRA for DM-electron interactions?

**OνDES Project**

**O**bservatory for **N**eutrino and **D**ark matter **E**lectron **S**cattering

## Main research goals of OνDES

DM-e scattering search

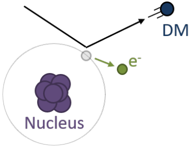

ν-e scattering search

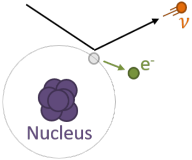

Migdal effect

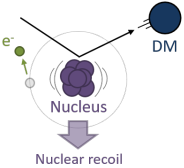

Figures by L. Ziegele

# Detector

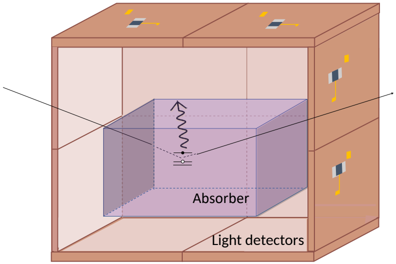

Figure by V. Zema

## Detection principle

- Particle interactions cause ionization or excitations of electrons within the absorber crystal (from valence band to conduction band)
- Relaxation by emission of photons with energy of the material-specific band gap
- Observable: single scintillation photons

# Detector

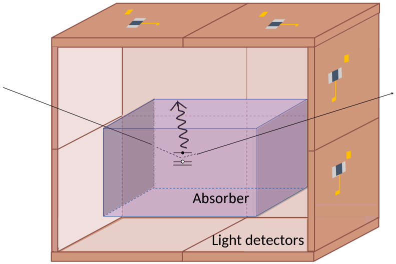

Figure by V. Zema

## Detection principle

- Particle interactions cause ionization or excitations of electrons within the absorber crystal (from valence band to conduction band)
- Relaxation by emission of photons with energy of the material-specific band gap
- Observable: single scintillation photons

## Requirements

- Low energy threshold of the light detectors of the order of the band gap (a few eV)
- High exposure for rare event searches
- Maximal scintillation light collection

# Research goals

## O$\nu$DES-DMe

Theoretical and experimental studies to search for DM-electron scattering using NaI CSCs*

- First studies on single photon detection: [Zema et al., 2024]
- Follow-up including excitons: [Taufertshöfer et al., 2026]

## O$\nu$DES-$\nu$e

Theoretical studies to search for solar neutrinos induced electronic excitations in NaI/GaAs CSCs*

## O$\nu$DES-ME

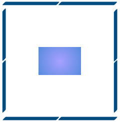

Theoretical and experimental studies to search for neutron or DM-induced Migdal effect using NaI CSCs*

---

* Cryogenic Scintillating Calorimeters

# Research goals

## O$\nu$DES-DMe

Theoretical and experimental studies to search for DM-electron scattering using NaI CSCs*

- First studies on single photon detection: [Zema et al., 2024]
- Follow-up including excitons: [Taufertshöfer et al., 2026]

## O$\nu$DES-$\nu$e

Theoretical studies to search for solar neutrinos induced electronic excitations in NaI/GaAs CSCs*

## O$\nu$DES-ME

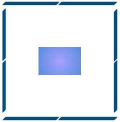

Theoretical and experimental studies to search for neutron or DM-induced Migdal effect using NaI CSCs*

---

* Cryogenic Scintillating Calorimeters

# Sensitivity

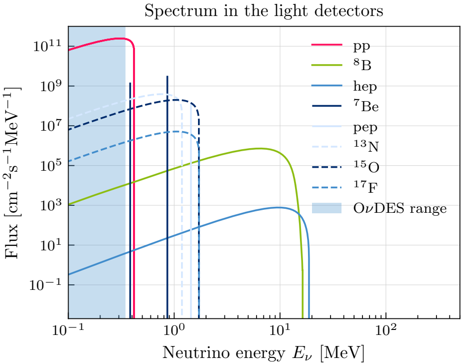

The pp chain has the right energy and the highest flux!

- Complementary information to Borexino on the pp chain
- Exploit high flux and low-energy sensitivity to study neutrino BSM* models with enhancement of the $\nu$-e scattering cross section at low energies

* Beyond the Standard Model

# Scattering rates

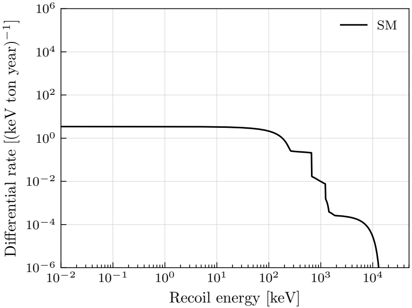

# Scattering rates

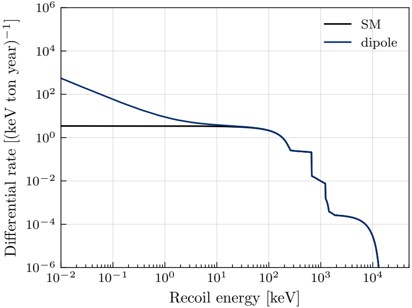

## Considered models [Schwemberger and Yu, 2022]

- Dipole moment neutrino

# Scattering rates

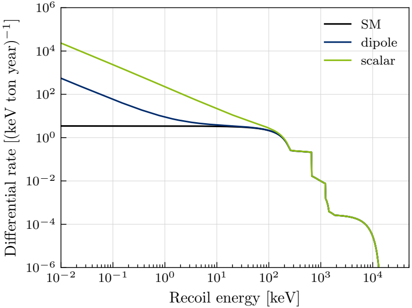

**Considered models** [Schwemberger and Yu, 2022]

- Dipole moment neutrino
- Simplified models for scalar,

# Scattering rates

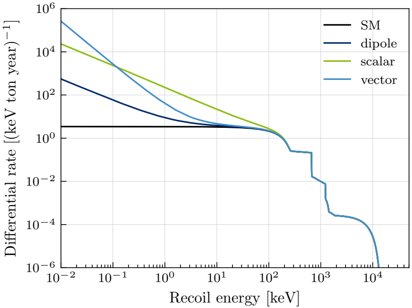

**Considered models** [Schwemberger and Yu, 2022]

- Dipole moment neutrino
- Simplified models for scalar, vector

# Scattering rates

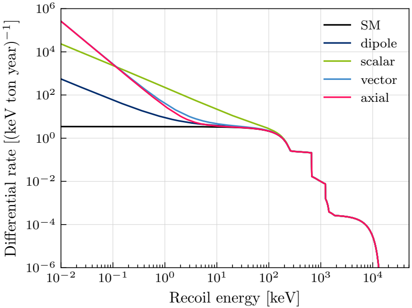

**Considered models** [Schwemberger and Yu, 2022]

- Dipole moment neutrino
- Simplified models for scalar, vector and axial vector mediator

# Scattering rates

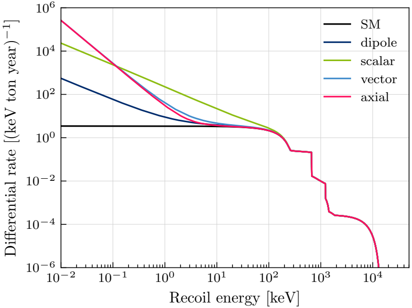

## Considered models [Schwemberger and Yu, 2022]

- Dipole moment neutrino
- Simplified models for scalar, vector and axial vector mediator

$$\frac{dR}{dE_e} = N_T \sum_{\nu_l} \int dE_\nu \frac{d\phi(E_\nu)}{dE_\nu} \; P(\nu_e \to \nu_l) \left( \frac{d\sigma(E_\nu, E_e)}{dE_e} \right)_{\nu_l}$$

# Scattering rates

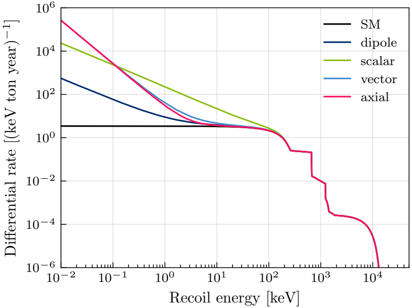

## Considered models [Schwemberger and Yu, 2022]

- Dipole moment neutrino
- Simplified models for scalar, vector and axial vector mediator

$$\frac{dR}{dE_e} = \underbrace{N_T}_{\text{number of target atoms}} \sum_{\nu_l} \int dE_\nu \frac{d\phi(E_\nu)}{dE_\nu} P(\nu_e \to \nu_l) \left( \frac{d\sigma(E_\nu, E_e)}{dE_e} \right)_{\nu_l}$$

# Scattering rates

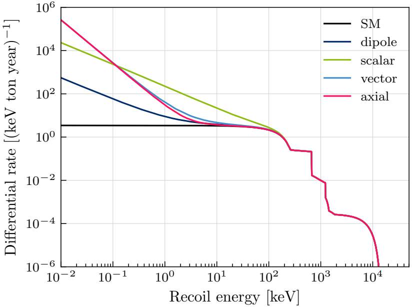

## Considered models [Schwemberger and Yu, 2022]

- Dipole moment neutrino
- Simplified models for scalar, vector and axial vector mediator

$$\frac{dR}{dE_e} = \underbrace{N_T}_{\text{number of target atoms}} \sum_{\nu_l} \int dE_\nu \overbrace{\frac{d\phi(E_\nu)}{dE_\nu}}^{\text{differential neutrino flux}} P(\nu_e \to \nu_l) \left(\frac{d\sigma(E_\nu, E_e)}{dE_e}\right)_{\nu_l}$$

# Scattering rates

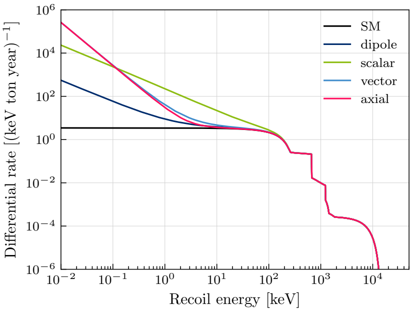

## Considered models [Schwemberger and Yu, 2022]

- Dipole moment neutrino
- Simplified models for scalar, vector and axial vector mediator

$$\frac{dR}{dE_e} = \underbrace{N_T}_{\text{number of target atoms}} \sum_{\nu_l} \int dE_\nu \overbrace{\frac{d\phi(E_\nu)}{dE_\nu}}^{\text{differential neutrino flux}} \underbrace{P(\nu_e \to \nu_l)}_{\text{oscillation probability}} \left(\frac{d\sigma(E_\nu, E_e)}{dE_e}\right)_{\nu_l}$$

# Scattering rates

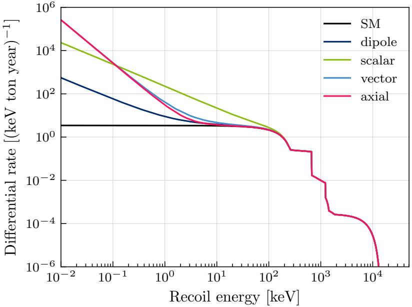

## Considered models [Schwemberger and Yu, 2022]

- Dipole moment neutrino
- Simplified models for scalar, vector and axial vector mediator

differential neutrino flux

differential cross section for the considered process

$$\frac{dR}{dE_e} = N_T \sum_{\nu_l} \int dE_\nu \frac{d\phi(E_\nu)}{dE_\nu} P(\nu_e \to \nu_l) \left( \frac{d\sigma(E_\nu, E_e)}{dE_e} \right)_{\nu_l}$$

number of target atoms

oscillation probability

# Electronic binding

- Can make different approximations to describe the electronic system in the detector (free or bound electrons or electronic bands)
- Our approach: consider atomic binding energy $B_i$ of the $i$-th atomic electron through stepping approximation:

$$\frac{d\sigma}{dE_e} \to \frac{1}{Z} \sum_{i=1}^{Z} \Theta(E_e - B_i) \frac{d\sigma}{dE_e}$$

- Good approximation for inner-shell electrons but full crystal treatment needed to properly model outer electrons that form bands

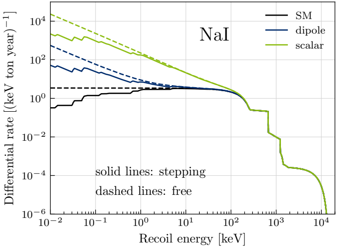

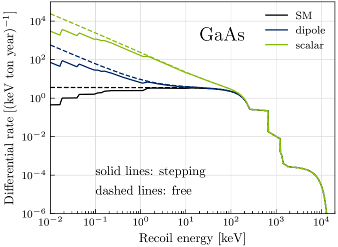

# Scattering off nuclei

- O$\nu$DES can also detect scintillation photons emitted following nuclear recoils
- Only a small part of the nuclear recoil energy excites electrons, most of it lost to phonons [Angloher et al., 2026]
- Amount of loss not know: no theoretical model or measurements at low energies, making calculation unreliable [Angloher et al., 2026]
- Our conservative approach for these sensitivities studies: ignore nuclear recoils

# Discovery projections

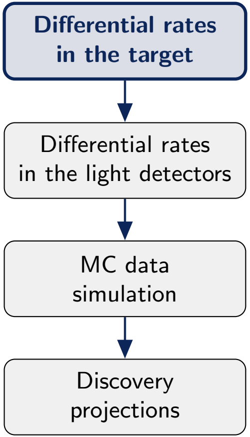

**Differential rates in the target**

Differential rates in the light detectors

MC data simulation

Discovery projections

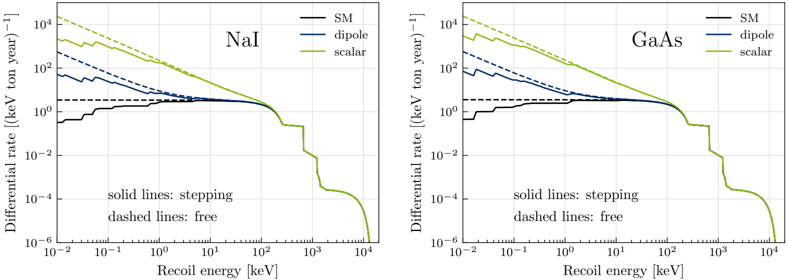

# Discovery projections

Differential rates in the target

**Differential rates in the light detectors**

MC data simulation

Discovery projections

- Observable: number of scintillation photons
- Translate deposited energy into number of emitted scintillation photons: [Zema et al., 2024]

$$n_\gamma = 1 + \left\lfloor \frac{E_e - \overbrace{E_g}^{\text{band gap energy}}}{\underbrace{\epsilon}_{\text{mean energy per electron-hole pair}}} \right\rfloor$$

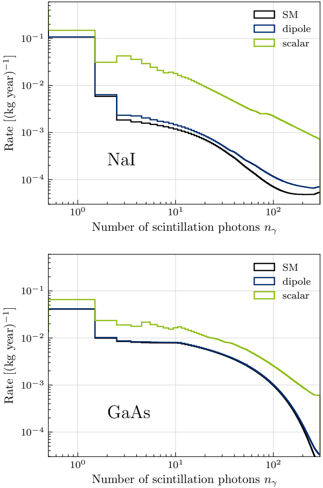

# Discovery projections

Differential rates in the target

**Differential rates in the light detectors**

MC data simulation

Discovery projections

- Consider the finite resolution of the light detectors, but an idealized perfect efficiency

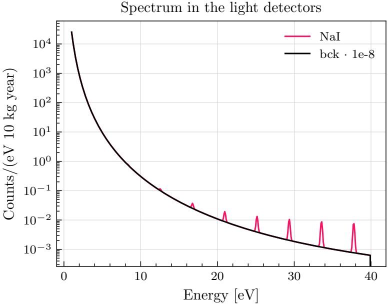

# Discovery projections

Differential rates in the target

**Differential rates in the light detectors**

MC data simulation

Discovery projections

- Consider the finite resolution of the light detectors, but an idealized perfect efficiency

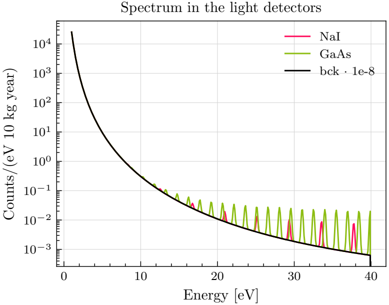

# Discovery projections

Differential rates in the target

↓

Differential rates in the light detectors

↓

**MC data simulation**

↓

Discovery projections

- Model the low-energy excess as measured in [Angloher et al., 2023] as background, and any neutrino signal (SM + BSM) as the potential signal
- For each configuration of mediator mass, coupling, exposure and background suppression, generate many random pseudo-datasets — reproducing the statistical fluctuations a real measurement would have

* MC = Monte Carlo

# Discovery projections

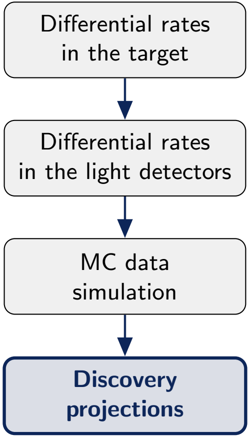

Differential rates in the target

Differential rates in the light detectors

MC data simulation

**Discovery projections**

- For each pseudo-dataset, check how distinguishable it looks from background alone
- For each fixed model, background and exposure, repeat for increasing couplings
- The smallest coupling for which the data is typically distinguishable from the background at 90% CL* corresponds to a point on the coupling-vs-exposure plot

---

* Confidence Level

# Discovery projections: results

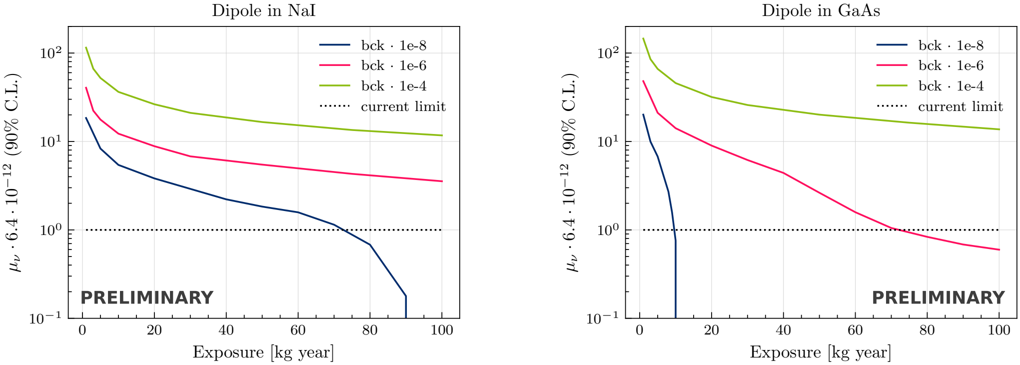

# Discovery projections: results

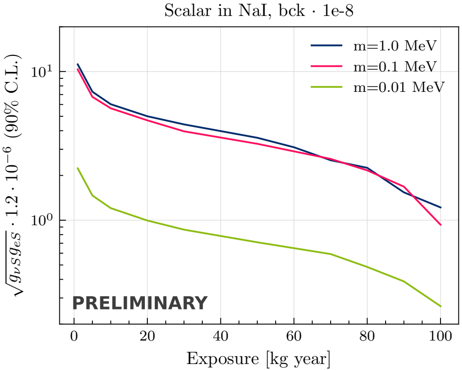

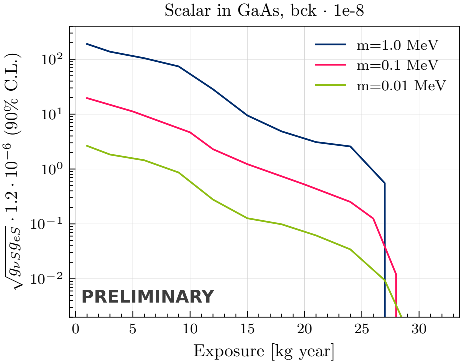

Note: The non-monotonic behavior of the curves at high exposures is probably due to statistical fluctuations in the MC - still under investigation

# Research goals

## O$\nu$DES-DMe

Theoretical and experimental studies to search for DM-electron scattering using NaI CSCs*

- First studies on single photon detection: [Zema et al., 2024]
- Follow-up including excitons: [Taufertshöfer et al., 2026]

## O$\nu$DES-$\nu$e

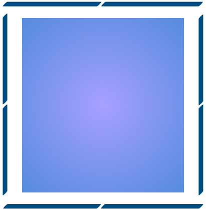

Theoretical studies to search for solar neutrinos induced electronic excitations in NaI/GaAs CSCs*

## O$\nu$DES-ME

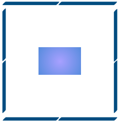

Theoretical and experimental studies to search for neutron or DM-induced Migdal effect using NaI CSCs*

* Cryogenic Scintillating Calorimeters

# Proof-of-principle prototype

- Topic of L. Ziegele's Master thesis within the COSINUS group at the Max Planck Institute for Physics [Ziegele, 2025]

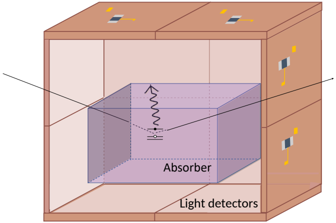

Figure by V. Zema

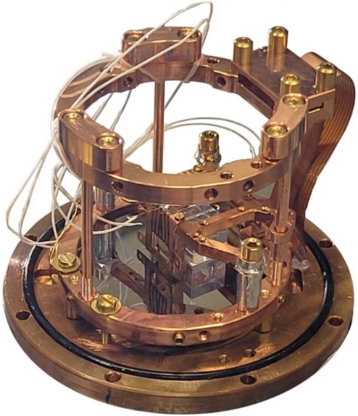

Figure by L. Ziegele

# Encouraging results

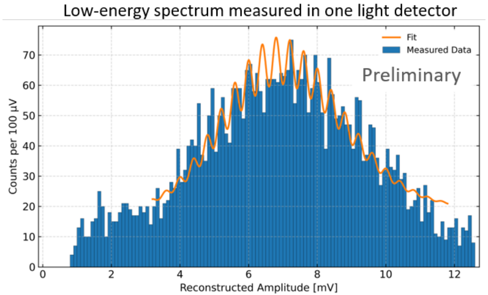

Figure from [Ziegele, 2026]

- Measured in COSINUS above-ground cryostat at the Max Planck Institute for Physics
- Indications of single-photon peaks
- Uncertainties because of low statistics and no reliable energy calibration at $\mathcal{O}$(eV) energies

# Conclusions

The O$\nu$DES project:

- Proposes a new CSC$^*$ detector design to probe DM-e ([Zema et al., 2024]) and $\nu$-e interactions (this work, paper in preparation)
- Proof-of principle prototype successful: long-term low-background run of full O$\nu$DES prototype planned at the COSINUS underground facility at LNGS underground lab
- Theoretical studies on the effect of excitons ([Taufertshöfer et al., 2026])
- Extension of the EXCEED-DM package to several crystal materials ([Andiné et al., 2026])
- Ongoing studies on the sensitivity of O$\nu$DES to DM induced Migdal effect, on the nature and possible mitigation of the low energy excess and the measurement of the experimental parameters relevant for this research, e.g. quenching factors

---

$^*$ Cryogenic Scintillating Calorimeters

# BACKUP

# Considered models

| Type | $\mathcal{L}$ | $\frac{d\sigma}{dE_e}$ | $\frac{d\sigma}{dE_N}$ |
|---|---|---|---|
| dipole | $\supset \mu_\nu \bar{\nu} \sigma^{\alpha\beta} \partial_\beta A_\alpha \nu$ | $\mu_\nu^2 \alpha \left( \frac{1}{E_e} - \frac{1}{E_\nu} \right)$ | $\mu_\nu^2 \alpha Z^2 F^2(E_N) \left( \frac{1}{E_N} - \frac{1}{E_\nu} \right)$ |
| scalar | $\supset g_{\nu S}\, \phi\, \bar{\nu}_R\, \nu_L + \text{h.c.}$ | $\frac{g_{\nu S}^2\, g_{eS}^2\, E_e\, m_e^2}{4\pi E_\nu^2\, (2E_e m_e + m_S^2)^2}$ | $\frac{F^2(E_N)\, Q_s'^2\, E_N\, m_N^2}{4\pi\, E_\nu^2\, (2E_N m_N + m_S^2)^2}$ |
| vector | $\supset g_{\nu V} \bar{\nu}_L \gamma^\mu \nu_L Z'_\mu$ | $\frac{\sqrt{2} G_F m_e g_v g_{\nu V} g_{eV}}{\pi(2E_e m_e + m_V^2)} + \frac{m_e g_{\nu V}^2 g_{eV}^2}{2\pi(2E_e m_e + m_V^2)^2}$ | $- \frac{F^2(E_N) G_F m_N Q_v Q_v' (2E_\nu^2 - E_N m_N)}{2\sqrt{2}\pi E_\nu^2 (2E_N m_N + m_V^2)}$<br>$+ \frac{F^2(E_N) m_N Q_v'^2 (2E_\nu^2 - E_N m_N)}{4\pi E_\nu^2 (2E_N m_N + m_V^2)^2}$ |
| axial vector | $\supset g_{\nu A}\, \bar{\nu}_L\, \gamma^\mu\, \nu_L\, Z'_\mu$ | $\frac{\sqrt{2} G_F m_e g_a g_{\nu A} g_{eA}}{\pi(2E_e m_e + m_A^2)} + \frac{m_e g_{\nu A}^2 g_{eA}^2}{2\pi(2E_e m_e + m_A^2)^2}$ | $\frac{F^2(E_N)\, G_F\, m_N\, Q_a' [Q_a (2E_\nu^2 + E_N m_N) - Q_v E_N E_\nu]}{2\sqrt{2}\pi E_\nu^2 (2E_N m_N + m_A^2)}$<br>$+ \frac{F^2(E_N)\, m_N\, Q_a'^2 (2E_\nu^2 + E_N m_N)}{4\pi E_\nu^2 (2E_N m_N + m_A^2)^2}$ |

Equations from [Schwemberger and Yu, 2022]

# Statistical treatment

- Use MC data simulated under the null hypothesis $\mathcal{H}_0$ of background only and the alternative hypothesis $\mathcal{H}_a$ of background + signal
- Use test statistics

$$q = \begin{cases} -2\ln\left(\frac{\mathcal{L}(\mathbf{d}_{\mathcal{H}}|g=0,\hat{\hat{\Theta}})}{\mathcal{L}(\mathbf{d}_{\mathcal{H}}|\hat{g},\hat{\Theta})}\right), & \hat{g} \geq 0 \\ 0, & \hat{g} < 0 \end{cases}$$

with the binned Poisson likelihood

expected number of events in bin *i*

$$\mathcal{L}(\mathbf{d}_{\mathcal{H}}|g,\Theta) = \prod_i \frac{e^{-\nu_i}}{n_i!}\nu_i^{n_i}$$

number of simulated events falling into bin *i*

- For each MC simulation, find $q_a$ by maximizing the likelihood
- The coupling we are looking for is the one corresponding to $q_a \simeq 1.63$, which corresponds to the 90% CL

# Quenching factor

- Defined as conversion factor of the nuclear recoil energy $E_N$ into the equivalent electron energy $E_e$:

$$E_e = Y(E_N)E_N$$

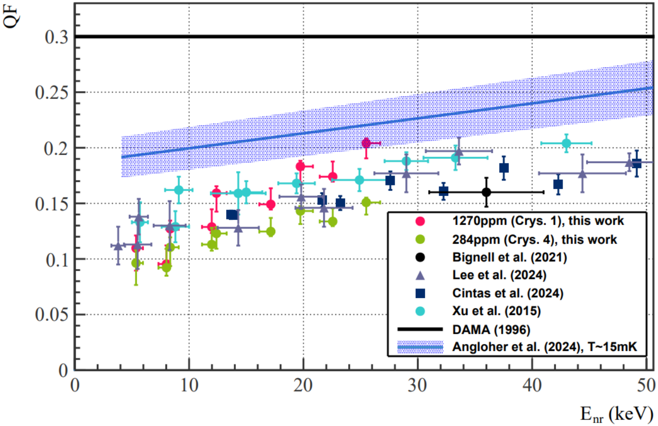

Comparison of different quenching factor measurements for Na. Taken from [Angloher et al., 2026].

# Origin of the multi-Gaussian peak

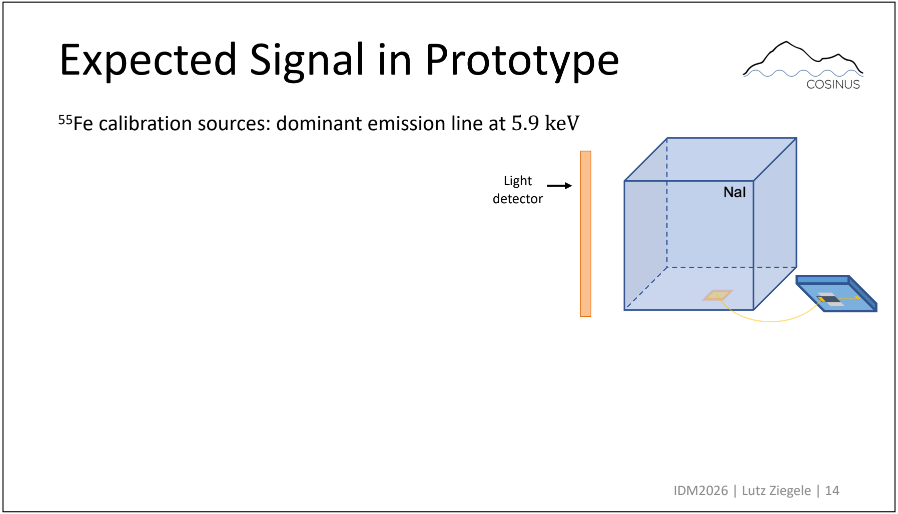

## Expected Signal in Prototype

$^{55}$Fe calibration sources: dominant emission line at 5.9 keV

IDM2026 | Lutz Ziegele | 14

# Origin of the multi-Gaussian peak

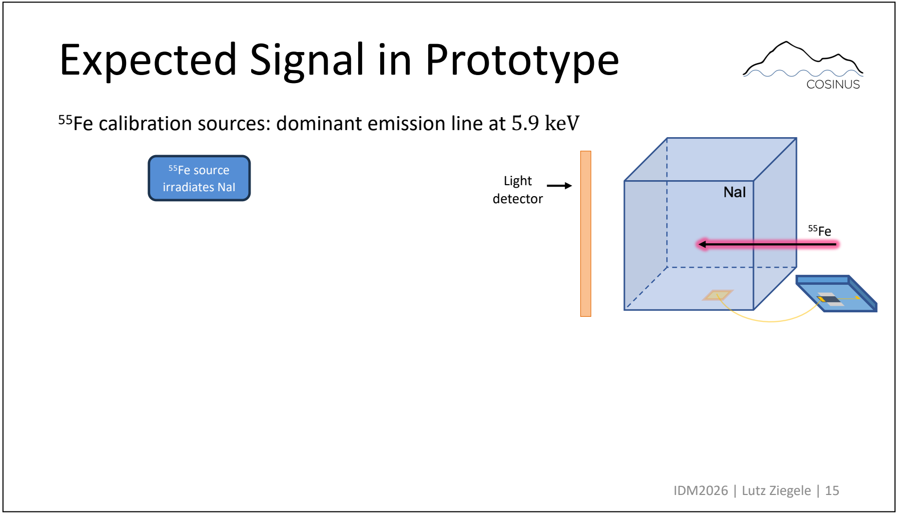

## Expected Signal in Prototype

$^{55}$Fe calibration sources: dominant emission line at 5.9 keV

$^{55}$Fe source irradiates NaI

IDM2026 | Lutz Ziegele | 15

# Origin of the multi-Gaussian peak

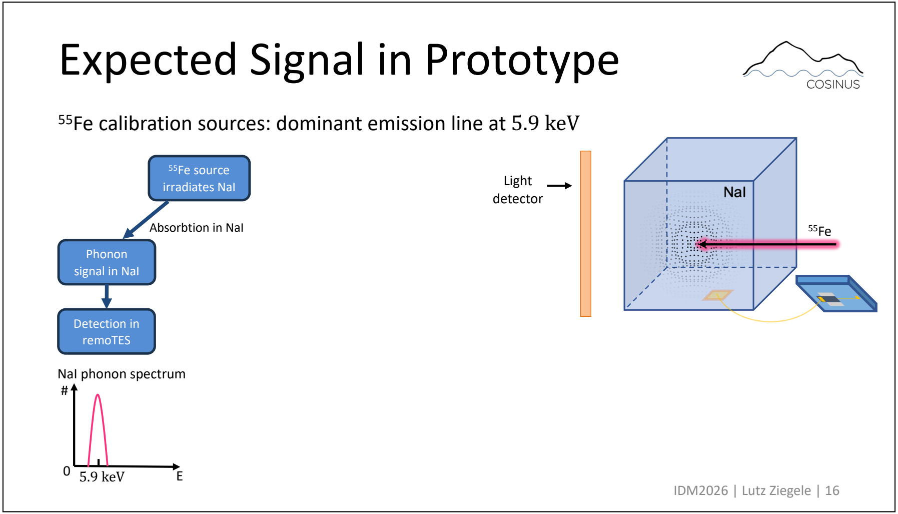

## Expected Signal in Prototype

$^{55}$Fe calibration sources: dominant emission line at 5.9 keV

$^{55}$Fe source irradiates NaI

Absorbtion in NaI

Phonon signal in NaI

Detection in remoTES

NaI phonon spectrum

IDM2026 | Lutz Ziegele | 16

# Origin of the multi-Gaussian peak

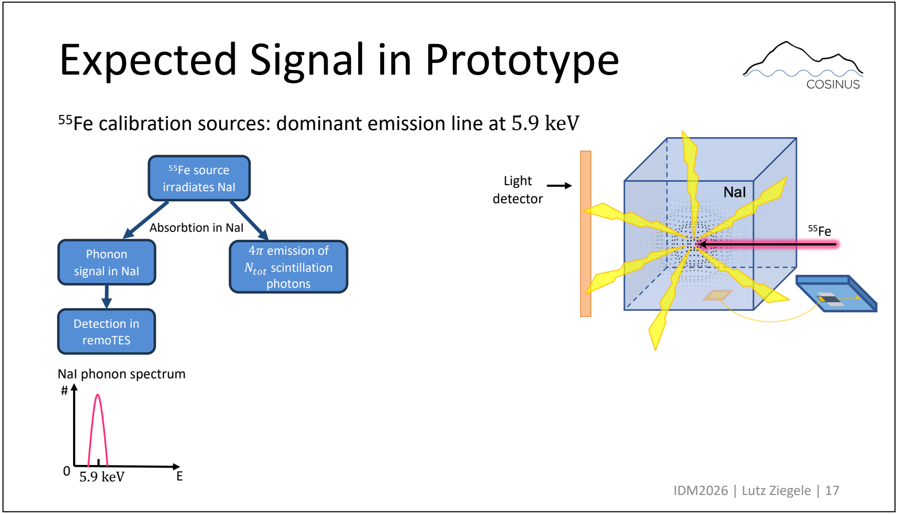

## Expected Signal in Prototype

$^{55}$Fe calibration sources: dominant emission line at 5.9 keV

$^{55}$Fe source irradiates NaI

Absorbtion in NaI

Phonon signal in NaI

Detection in remoTES

$4\pi$ emission of $N_{tot}$ scintillation photons

IDM2026 | Lutz Ziegele | 17

# Origin of the multi-Gaussian peak

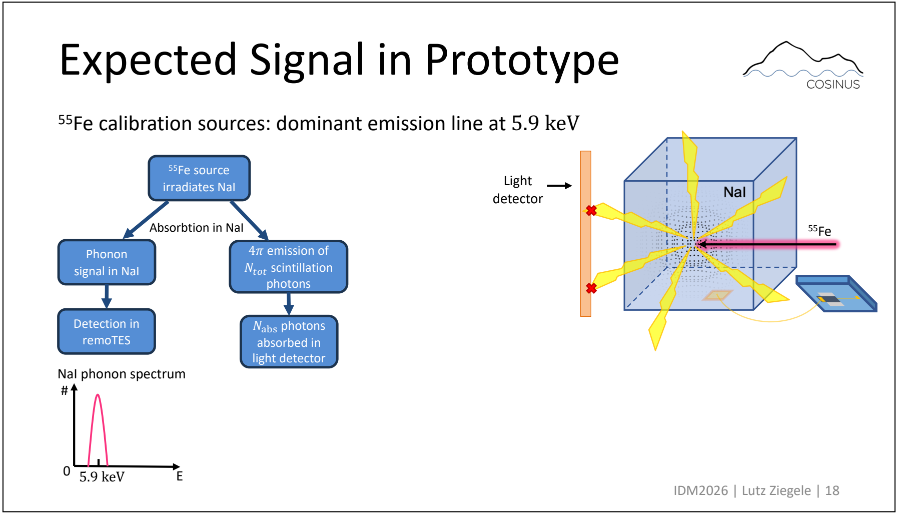

## Expected Signal in Prototype

$^{55}$Fe calibration sources: dominant emission line at 5.9 keV

$^{55}$Fe source irradiates NaI

Absorbtion in NaI

Phonon signal in NaI

Detection in remoTES

4$\pi$ emission of $N_{tot}$ scintillation photons

$N_{\text{abs}}$ photons absorbed in light detector

NaI phonon spectrum

IDM2026 | Lutz Ziegele | 18

# Origin of the multi-Gaussian peak

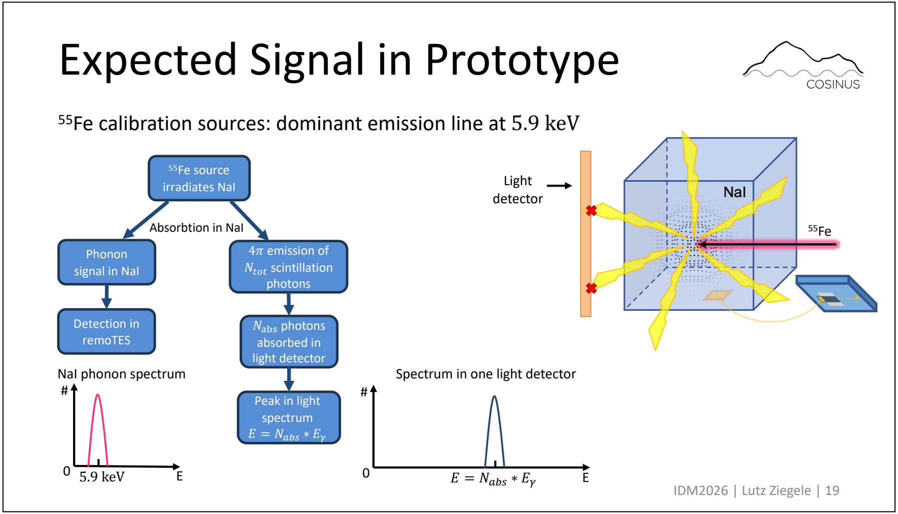

## Expected Signal in Prototype

$^{55}$Fe calibration sources: dominant emission line at 5.9 keV

- $^{55}$Fe source irradiates NaI
- Absorbtion in NaI
- Phonon signal in NaI → Detection in remoTES
- $4\pi$ emission of $N_{tot}$ scintillation photons → $N_{\text{abs}}$ photons absorbed in light detector → Peak in light spectrum $E = N_{abs} * E_{\gamma}$

NaI phonon spectrum

Spectrum in one light detector

IDM2026 | Lutz Ziegele | 19

# Origin of the multi-Gaussian peak

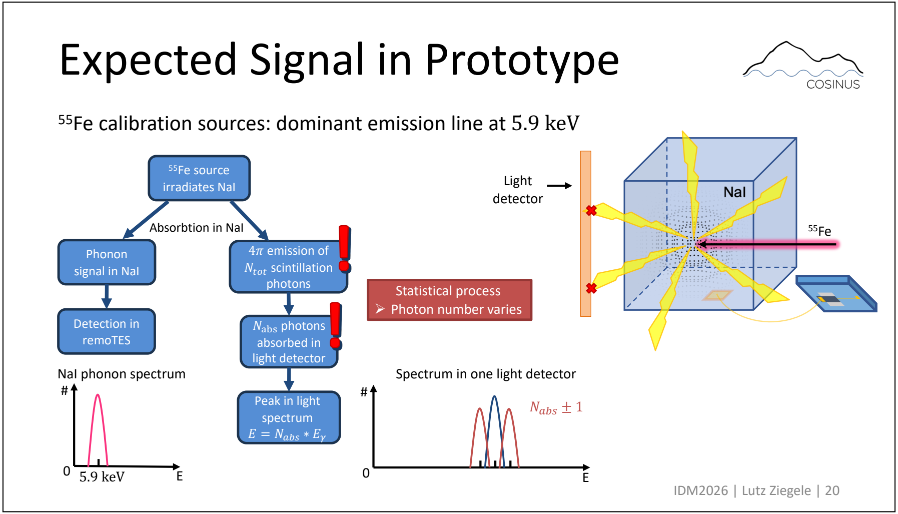

## Expected Signal in Prototype

COSINUS

$^{55}$Fe calibration sources: dominant emission line at 5.9 keV

$^{55}$Fe source irradiates NaI

Absorbtion in NaI

Phonon signal in NaI

Detection in remoTES

$4\pi$ emission of $N_{tot}$ scintillation photons

$N_{abs}$ photons absorbed in light detector

Peak in light spectrum $E = N_{abs} * E_{\gamma}$

Statistical process
➢ Photon number varies

IDM2026 | Lutz Ziegele | 20

# Origin of the multi-Gaussian peak

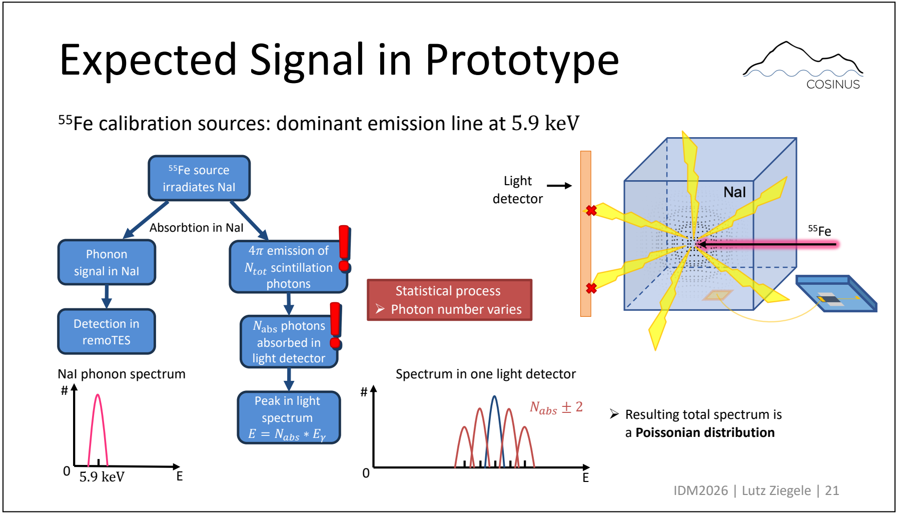

## Expected Signal in Prototype

$^{55}$Fe calibration sources: dominant emission line at 5.9 keV

$^{55}$Fe source irradiates NaI

Absorbtion in NaI

Phonon signal in NaI

Detection in remoTES

$4\pi$ emission of $N_{tot}$ scintillation photons

$N_{abs}$ photons absorbed in light detector

Peak in light spectrum $E = N_{abs} * E_{\gamma}$

Statistical process
- ➢ Photon number varies

- ➢ Resulting total spectrum is a **Poissonian distribution**

IDM2026 | Lutz Ziegele | 21

# Origin of the multi-Gaussian peak

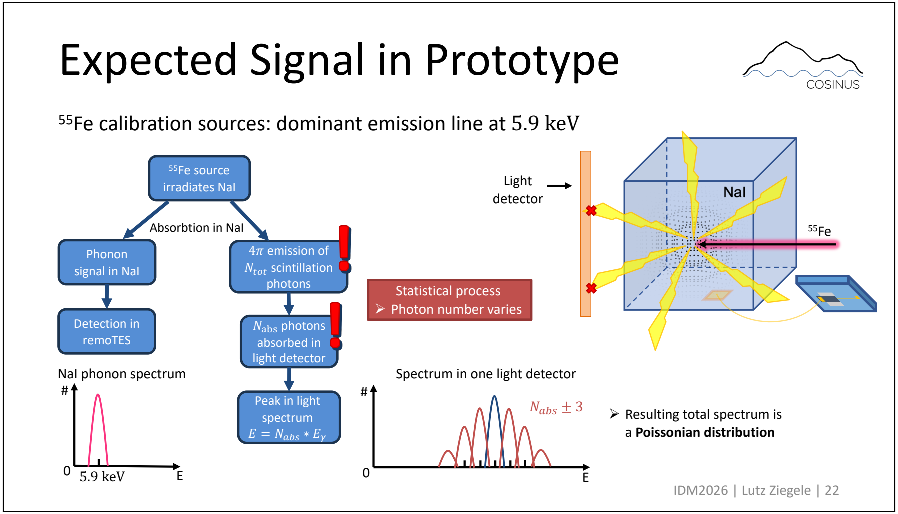

## Expected Signal in Prototype

COSINUS

$^{55}$Fe calibration sources: dominant emission line at 5.9 keV

$^{55}$Fe source irradiates NaI

Absorbtion in NaI

Phonon signal in NaI

Detection in remoTES

$4\pi$ emission of $N_{tot}$ scintillation photons

$N_{abs}$ photons absorbed in light detector

Peak in light spectrum $E = N_{abs} * E_{\gamma}$

Statistical process
➢ Photon number varies

➢ Resulting total spectrum is a **Poissonian distribution**

IDM2026 | Lutz Ziegele | 22

# Origin of the multi-Gaussian peak

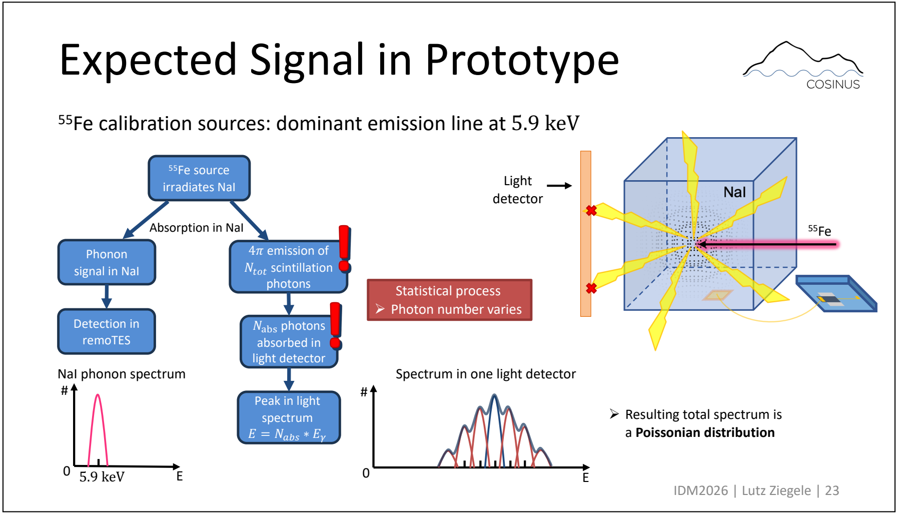

## Expected Signal in Prototype

COSINUS

$^{55}$Fe calibration sources: dominant emission line at 5.9 keV

$^{55}$Fe source irradiates NaI

Absorption in NaI

Phonon signal in NaI

Detection in remoTES

$4\pi$ emission of $N_{tot}$ scintillation photons !

$N_{\text{abs}}$ photons absorbed in light detector !

Peak in light spectrum $E = N_{abs} * E_{\gamma}$

Statistical process

- ➢ Photon number varies

Light detector

NaI

$^{55}$Fe

NaI phonon spectrum

#

0

5.9 keV

E

Spectrum in one light detector

#

0

E

- ➢ Resulting total spectrum is a **Poissonian distribution**

IDM2026 | Lutz Ziegele | 23

# References I

Andiné, E., Ax, J., Catena, R., Hjelseth, P., Ingvast, J., Johansson, E., et al. (2026).

Angloher, G., Banik, S., Benato, G., Bento, A., Bertolini, A., Breier, R., et al. (2023).
Results on sub-GeV dark matter from a 10 eV threshold CRESST-III silicon detector.
*Phys. Rev. D*, 107:122003.

Angloher, G., Bharadwaj, M., Böhmer, A., Cababie, M., Colantoni, I., Dafinei, I., Marco, N. D., Dittmar, C., Einfalt, L., Ferella, F., et al. (2026).
Quenching factors for na recoils as a function of tl dopant concentrations in nai (tl) crystals.
*The European Physical Journal C*, 86(5):485.

Schwemberger, T. and Yu, T.-T. (2022).
Detecting beyond the standard model interactions of solar neutrinos in low-threshold dark matter detectors.
*Phys. Rev. D*, 106:015002.

# References II

Taufertshöfer, N., Zema, V., Catena, R., Olevano, V., and Spaldin, N. A. (2026).
Excitonic contributions to dark matter-electron scattering.
*Phys. Rev. Res.*, 8:013056.

Zema, V., Figueroa, P., Angloher, G., Bharadwaj, M. R., Frank, T., Hughes, M. N., et al. (2024).
Dark matter-electron scattering search using cryogenic light detectors.
*Phys. Rev. D*, 110:123012.

Ziegele, L. (2025).
Development of Cryogenic Single-Photon Detectors to Study the Light Output of Sodium Iodide Crystals for Rare Event Searches.
Master's thesis, Technical University of Munich and Max Planck Institute for Physics.

Ziegele, L. (2026).
Development of Cryogenic Single-Photon Detectors to Study the Light Output of Sodium Iodide Crystals for Rare Event Searches.
Talk at IDM 2026.